

Precipitation, temperature and wind in Norway: dynamical downscaling of ERA40

I. Barstad · A. Sorteberg · F. Flatøy ·
M. Déqué

Received: 21 April 2008 / Accepted: 30 September 2008
© Springer-Verlag 2008

Abstract A novel downscaling approach of the ERA40 (ECMWF 40-years reanalysis) data set has been taken and results for comparison with observations in Norway are shown. The method applies a nudging technique in a stretched global model, focused in the Norwegian Sea (67°N, 5°W). The effective resolution is three times the one of the ERA40, equivalent to about 30 km grid spacing in the area of focus. Longer waves ($<T42$) in the downscaled solution are nudged towards the ERA40 solution, and thus the large-scale circulation is similar in the two data sets. The shorter waves are free to evolve, and produce high intensities of winds and precipitation. The comparison to observations incorporate numerous station data points of (1) precipitation (#357), (2) temperature (#98) and (3) wind (#10), and for the period 1961–1990, the downscaled data set shows large improvements over ERA40. The daily precipitation shows considerable reduction in bias (from 50 to 11%), and twofold reduction at the 99.9 percentile (from –59 to –29%). The daily temperature showed a bias reduction of about a degree in most areas, and relative large RMSE reduction (from 7.5 to 5.0°C except winter). The wind comparison showed a slight improvement in bias, and significant improvements in RMSE.

1 Introduction

Time series of the atmospheric state have laid down building blocks in our understanding of the atmosphere and produced many revelations useful for mankind. For instance, discovery of physical mechanisms in the atmosphere may help us to a better understanding of the climate system and consequently improve the basis for decision-making. Understanding of such mechanisms will be needed in order to infer impacts of future climates.

The reanalyses from National Centres for Environmental Prediction (NCEP/NCAR, Kalnay et al. 1996) and European Centre for Medium Range Forecasts (ECMWF, Kållberg et al. 2004; hereafter ERA40) are together with the point observations our best estimate of the atmospheric state. Both reanalysis datasets extend over several decades and a vast amount of observations has been assimilated into the respective model systems. However, to some extent it deviates from the true, unknown state and the large scales are best described, simply because they are better sampled by the observational network and the resolution of the data assimilation systems. Details on scales of 100 km or less are insufficiently sampled and subject to significant uncertainty. In this regard, the shortcomings in the reanalyses have been studied by Caires and Sterl (2003), Caires et al. (2004), Smith et al. (2001), Jiang et al. (2005) and Yuan (2004).

Extreme events of wind, temperature and precipitation, have generally large impacts on human society and biological life. Droughts, floods and cold spells are examples of potentially devastating anomalies. Significant statistics of extremes demand long time series in order to have a sufficient data foundation. A large data set will give increased degrees of freedom and thereby narrow confidence intervals. When it comes to data from models, the

I. Barstad (✉) · A. Sorteberg · F. Flatøy
Bjerknes Centre for Climate Research, Allegt.55,
5007 Bergen, Norway
e-mail: Idar.Barstad@bjerknes.uib.no

M. Déqué
EAC/GMGEC/CNRM, Météo France, 42 Ave Coriolis,
31057 Toulouse, France

intensity in the data series reflects the spatial and temporal model resolution, and thus for many purposes the resolution of the reanalyses is not enough.

There is a large body of literature where reanalyses have been used to produce datasets with improved representation of smaller scales. Different regionalization methods, including high-resolution and variable resolution AGCMs (Déqué and Piedelievre 1995), nested regional climate models, or RCMs (Giorgi and Mearns 1999), and statistical downscaling (Wilby et al. 1998) have been employed. RCM models are driven by lateral boundary and sea surface conditions from a reanalysis or coupled ocean–atmosphere GCM projection, while the AGCM only needs the sea surface conditions as input.

Schmidli et al. (2006) and Schmidli et al. (2007) present results from a study where precipitation data from statistical downscaling models (SDMs) and RCMs are compared to ERA40 reanalysis and future (2071–2100) climate. Their main findings indicate that all models are capable of reducing the large biases in the precipitation frequency distribution, intensity and magnitude. Over flat terrain and in summer, the differences between the RCMs and SDMs are small, but for difficult situations, e.g. in winter and over complex terrain, the better RCMs achieve significantly higher skills than SDMs. Clear differences are also seen when correlations in year-to-year anomalies are considered, where SDMs strongly underestimate the magnitude of the variations.

Both Jacob et al. (2007) and Fowler et al. (2007) report from the European project PRUDENCE (Christensen et al. 2002) where nine different RCMs and one variable resolution AGCM are used to produce present-day climate and climate-change simulations for Europe. The AGCM is the same model as used in our study but with lower vertical resolution (31 vs. 60 levels) and stretching factor (2.5 vs. 3).

The analysis in Jacob et al. (2007) focuses on temperature and precipitation and reports that the large-scale circulation of the driving global climate model (GCM) are reproduced in the RCM results except for some locations where large differences between regional biases in surface temperature and precipitation occur.

Fowler et al. (2007) investigates how the formulations of global and regional climate models contribute to the scenario uncertainty. When looking at changes to precipitation extremes over Europe by 2070–2100 under the SRES A2 emissions scenario, they find that all RCMs project increases in the amount of extreme precipitation for most of Europe. The changes are strongly influenced by the driving GCM, but moderated by the RCM, which also influences the spatial pattern.

The rest of this paper is organized as follows: Sect. 2 describes the method used for the downscaling. In Sect. 3,

comparisons of wind, precipitation and temperature from the downscaling, ERA40 dataset and observations are found. With Sect. 4, we conclude the paper.

2 Method

2.1 The nudging technique

To date, in most regional dynamical downscaling studies performed, the forcing is administered exclusively at the lateral boundaries of regional models. The boundary relaxation scheme effectively damps small-scale discrepancies that accumulate in the vicinity of the outflow boundaries, but it does not necessarily handle larger scales correctly, and the long waves may reflect and interfere within the domain. The problem of only imposing the large scales on the boundaries has become more apparent as experiences with regional climate models have grown during the last decade. In a predictability study, Vukicevic and Errico (1990) showed that most of the error growth in a regional model occurred in wavelengths longer than 2,000 km. Extreme events are often related to both the occurrence of a certain large-scale circulation pattern, long-range transport of water vapor and to an enhancement of the event due to local effects like topography or convection. To incorporate these local features in a physically consistent way with the large-scale circulation pattern, we propose to use selective spectral nudging (Waldron et al. 1996) in a global model with a stretched grid configuration. The nudging will provide large-scale flow consistent with the large-scale reanalysis circulation, but let the model freely develop small-scale features related to topography and local scale circulation patterns. The approach has been used in several regional models (von Storch et al. 2000; Weisse and Feser 2003; Meinke et al. 2004; Miguez-Macho et al. 2004) where it has been shown to give added value and eliminate the sensitivity of regionally downscaled precipitation patterns to the choice of model domain and grid geometry (Miguez-Macho et al. 2005).

The nudging technique is simply a Newtonian relaxation, where part of the model solution is nudged toward the reanalysis values every time step. The Arpege/IFS system is well suited for doing the spectral nudging since it shares the same dynamical core and vertical coordinate system as the ERA40 reanalysis. To reduce errors related to vertical interpolations, the model is run with the same vertical levels as the ERA40 (60 levels). The reanalysis is available in spectral space on its original resolution every 6 h, and are linearly interpolated to the stretched grid configuration and to models time step (10 min). Thus, in the continuous integration the interpolated reanalysis values are gradually assimilated into the model. The nudging is done in spectral space where the spectral coefficients, corresponding to

particular wave lengths, are nudged with given amplitude up to wave number T42, and the relaxation time decrease towards zero at T51. For larger wave numbers, the solutions are free to develop.

$$\frac{\partial X}{\partial t} = \frac{\partial X_{\text{MODEL}}}{\partial t} + \frac{1}{\tau} (X_{\text{REANALYSIS}} - X_{\text{MODEL}}) \quad (1)$$

where τ is the relaxation time and X the prognostic variable. In the current experiment, we apply nudging for divergence ($\tau = 48$ h), vorticity ($\tau = 6$ h), temperature ($\tau = 24$ h), ln of the surface pressure ($\tau = 24$ h) and surface temperature ($\tau = 48$ h) equally for the whole model domain. The nudging approach is the same as the successful one taken in Guldberg et al. (2005).

The use of a global model prevents problems related to the treatment of lateral boundaries and ensures that the source of water vapor is inside the model domain. Also the problems of moisture spin up will be eliminated because the model is allowed to evolve without any re-initialization throughout the experiment. The stretched grid configuration has a sensitivity to the cumulus parameterization in the tropics (more precipitation for higher resolutions), but for the relevant area our set-up has similar resolution as the standard so additional tuning is not necessary. Further notices on resolution sensitivities may be found in Lorant and Royer (2001).

2.2 Comparison of meteorological parameters

We have chosen to compare our downscaling results to daily precipitation, temperature and wind for the period 1961–1990. These variables are the ones measured most widely and frequently in Norway, and thus provide the largest body of data for comparison.

In relation to the comparison of 10 m wind, we generally find the observations to have a very local representation, typically dominated by local valley flows or winds in small fjords systems. These will naturally not be a good comparison for the modeled wind. An exception is the coastal wind stations that typically have much improved representativity. We have identified ten stations somewhat evenly distributed along the coast. From experience, these stations are believed to have relatively high representativity (Pers. com. K. Harstveit, met.no) with homogeneous timeseries. These wind stations are: Lyngøy, Lindesnes, Obrestad, Flesland, Vigra, Ørlandet, Bodø, Andøya, Makkaur and Vardø, see Fig. 1 for geographical reference.

The precipitation stations—totally 357—are categorized in 13 different precipitation regions in Norway, see Fig. 3. These regions have been established through experience and investigations at the national meteorological institute (Hanssen-Bauer et al. 1997). We define wet days as those



Fig. 1 The terrain in the two systems. *Upper*: ERA40 (e4) and *lower*: Arpege (arpN). The counter interval is 100 m, starting at 100 m elevation. The stations used for wind comparison are indicated in the *upper panel*: Lyngøy (Ly), Lindesnes (Li), Obrestad (Ob), Flesland (Fl), Vigra (Vi), Ørlandet (Ør), Bodø (Bo), Andøya (An), Makkaur (Ma) and Vardø (Va), see Sect. 2.2

where precipitation amounts are above 0.1 mm in both the compared datasets, and in our comparisons, we only apply wet days.

For 2 m temperatures, we have applied a constant lapse rate of 6 K/km in order to adjust for terrain height differences between the model systems and observations. Assuming a constant lapse rate and thereby neglecting temperature effects from boundary layers etc. is far from perfect, but to first order, it will give a more fair comparison. Temperature stations have also been categorized in six temperature regions in Norway, similarly defined based on experience, (Hanssen-Bauer and Førland 1998). The six regions are—from south to north: Østlandet (southeastern area), Vestlandet (southwestern coast), Trøndelag (mid area), Nordland/Troms (northern coastal area), Finnmarksvidda (northern inner area) and Varanger (northeastern coast). For this parameter, there are totally 98 stations taken into consideration.

3 Results

In this paper, we center our attention of the information added to the reference dataset (ERA40; e4) by our downscaling simulation (nudged Arpege; arpN). From the

improved resolution in arpN, we first of all expect terrain features such as orographic precipitation and coastal jets to be more pronounced. Figure 1 indicates the terrain resolution for the two systems, and the tallest mountain in arpN is about double the one in e4. Phenomena on the open waters will typically be better resolved giving sharper gradients in fronts etc. and thus higher winds. A more detailed coastline will also give rise to differences.

The basis for the results and discussions in this study will be the three parameters mentioned in the previous section. The main emphasis is placed on extremes of precipitation and to some extent wind as these parameters obviously have a large direct impact on human and biological life. We will first make use of point measurements in the comparison, and then indicate how the geographical details look for the new downscaled data set.

3.1 Precipitation: point measurements

In the simulation of precipitation, arpN does a good job compared to e4 dataset. Figure 2 shows fitted gamma probability density function (PDF) based on all 357 precipitation stations, and we see that the arpN dataset has a significantly improved precipitation amount. The figures in Table 1 indicates that the percentage errors are much improved for higher percentile values.

In order for us to see more of the regional performance of the downscaling, we now turn to the defined precipitation regions (RR-region) in Norway as indicated on Fig. 3. We first look at the false alarm rate (FAR) for arpN which is about 30–40% in most regions and the hit rate (H) which is about 75%. The two regions 7 and 12 which both are rather dry deviate from this picture having H \sim 65% and

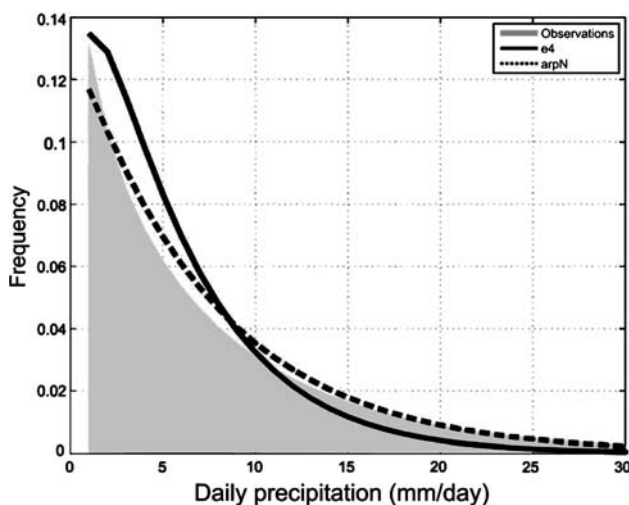


Fig. 2 Normalized frequency distribution of all precipitation stations (#357) that are included in the comparison. A gamma function fitted to the data, (gray): observations, (solid): e4 and (broken): arpN

Table 1 The relative error for model versus observations in % for different percentiles

Percentile (%)	Daily precipitation	
	e4	arpN
50	−53.1	−11.6
95	−45.3	−20.3
99	−51.4	−24.6
99.9	−58.4	−29.1

All precipitation stations are considered. Negative sign indicates underestimation by the model at given percentile. arpN is the nudged simulation and e4 is the ERA40 reference simulation

FAR \sim 44%. Furthermore, from Table 2 showing percentile for various RR-regions, and we see that the model has an underestimation of about 15–20% in most regions, less in dryer regions. For extreme precipitation events (99.9%), the underestimation is typically large, around 30% for regions with a strong orographic precipitation component (i.e. 4, 5, 6 and 8). Looking at the number of wet days in arpN, it varies at about 135% for the various regions, a 35% overestimation. In comparison, e4 has about 150% as the highest values (dry regions). We may conclude that the arpN simulation has similar deficiencies as other GCM model results (e.g. Mavromatis and Jones 1999), raining too often and too little, however this type of errors is significantly reduced compared to e4.

3.2 Precipitation: geographical distribution

In Fig. 3, we present the median (50 percentile) precipitation in Norway as it is produced by arpN. The mountainous regions facing west receive the largest amounts of precipitation. The pattern formed by the strong precipitation gradient between the windward and the lee side of the mountains is very similar to the gridded observational dataset from met.no (Tveito et al. 2005, not shown). Dry areas like 7 and 12 are nicely reproduced.

Extreme precipitation (99.9%) is shown in Fig. 3b). This level is equivalent to about the strongest precipitation day in 3 years. From Table 2, we see the underestimation at this level is about 30%. To achieve a simple bias correction for Fig. 3b), we make use of the information in Table 2. The simple correction is done by multiplying by the inverse of the simulated fraction. For 31% underestimation at an area (region 3 in Table 2) of about 40 mm/day (from Fig. 2), this is: $40(\text{mm/day})/(100\% - 31\%) = 58(\text{mm/day})$. Thus for region 3, we expect the 99.9 percentile of daily precipitation to be more like 58 mm rather than the depicted value, 40 mm. For many purposes, a more sophisticated adjustment scheme would be justified.

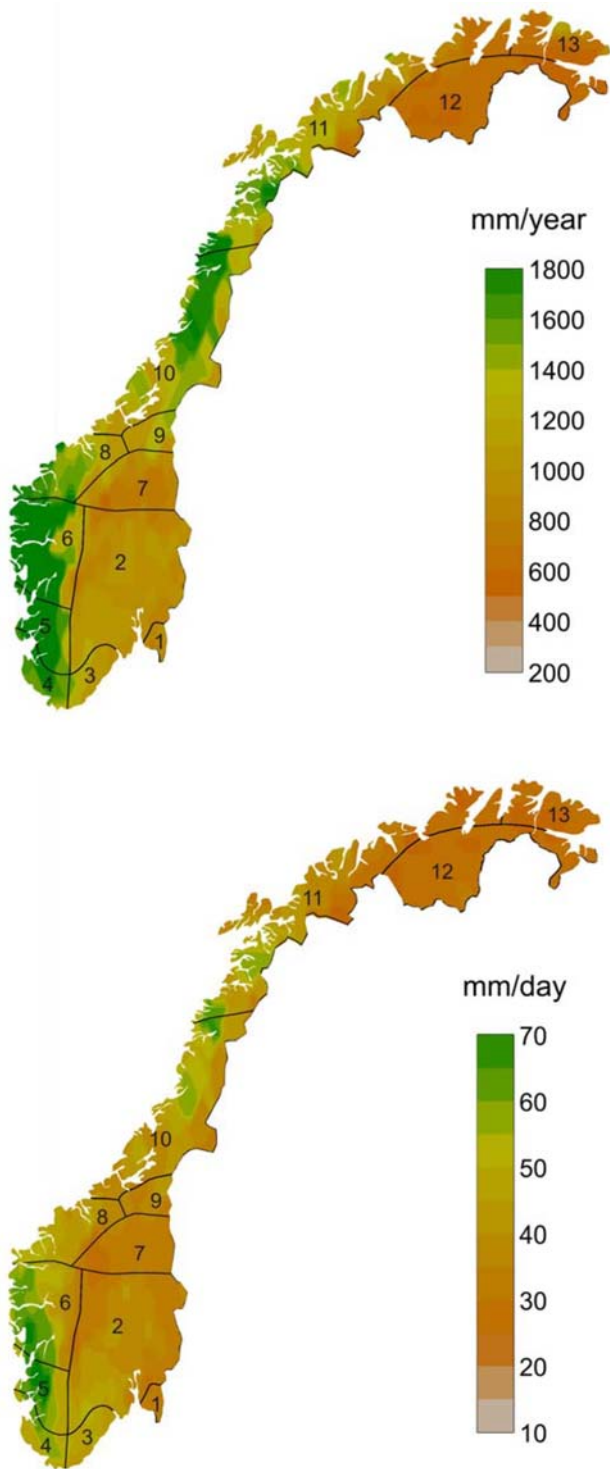


Fig. 3 **a** Mean precipitation as simulated by the arpN and **b** map of the 99.9 percentile. Precipitation regions are indicated

When comparing the geographical distribution in the two data sets (not shown), we find that arpN has improved precipitation amounts at the 50% percentile level in the southwestern coast and mid part of Norway. For the northern part, there is much less of a difference. This is due

Table 2 Similar to Table 1, but arpN is compared to observations in precipitation regions (indicated in Fig. 3)

RR-regions	Wet days (%)	50%	95%	99%	99.9%
1	138.8	-20.5	-23.1	-19.6	-15.2
2	147.0	-13.0	-17.6	-18.5	-17.2
3	139.5	-28.4	-28.7	-30.6	-31.0
4	126.4	-22.3	-22.8	-24.6	-27.0
5	127.7	-14.7	-16.6	-17.6	-18.7
6	125.7	-13.0	-24.5	-28.1	-33.2
7	156.4	3.4	-7.4	-7.1	-8.9
8	138.1	-10.7	-19.7	-25.3	-34.7
9	131.3	-4.3	-4.5	-10.0	-6.1
10	121.5	-10.1	-13.5	-17.7	-26.1
11	136.1	2.9	-3.1	-16.6	-37.3
12	147.0	6.6	-15.9	-18.1	-17.6
13	132.2	29.8	42.8	17.7	-7.4
Overall	135.0	-11.6	-20.3	-24.6	-29.1

Over/under estimation is indicated by (±) for different percentiles

to lesser precipitation in this area, and thus lesser chance for large deviations. For higher percentiles (e.g. 99.9), there is still a large difference in the south and much less in the north.

3.3 Temperature

The adjusted 2 m temperature (Sect. 2.2) is very well simulated. Figure 4 shows the fitted normal PDF for non-coastal stations in Norway. From the figure, we see that arpN distribution is close to the observed one. In a similar figure, but only for coastal stations (not shown), the arpN distribution

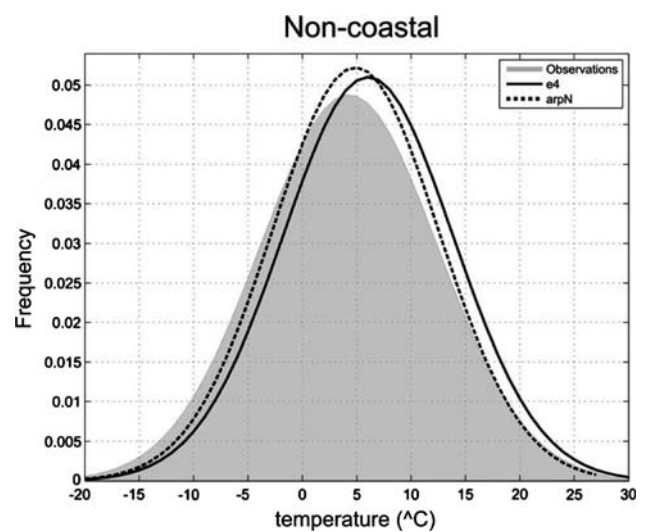


Fig. 4 Fitted normal distribution of daily temperature for non-coastal temperature stations in Norway for (*gray*): observation, (*solid*): ERA40 and (*broken*): arpN

Table 3 Temperature bias and RMSE for different temperature regions (see Sect. 2.2) in Norway, categorized in various seasons

T-reg.	Bias arpN				Bias e4			
	DJF	MAM	JJA	SON	DJF	MAM	JJA	SON
1	1.0	0.54	0.72	0.41	1.84	1.86	1.98	1.48
2	0.75	0.34	0.65	0.32	1.78	1.78	1.93	1.47
3	0.93	0.45	0.66	0.37	1.82	1.84	1.93	1.46
4	0.96	0.45	0.59	0.32	1.81	1.84	1.89	1.45
5	0.95	0.46	0.65	0.35	1.87	1.87	1.89	1.45
6	0.96	0.48	0.63	0.35	1.83	1.85	1.89	1.43

T-reg.	RMSE arpN				RMSE e4			
	DJF	MAM	JJA	SON	DJF	MAM	JJA	SON
1	14.7	5.1	3.9	6.9	16.4	7.5	7.1	8.3
2	13.8	5.0	3.9	6.7	15.5	7.1	6.9	8.1
3	14.5	5.0	3.8	7.1	16.4	7.3	6.9	8.5
4	15.1	5.4	3.8	6.7	16.5	7.6	6.6	8.1
5	14.7	4.9	3.7	7.2	16.7	7.3	6.7	8.5
6	14.4	4.9	3.7	7.1	16.2	7.1	6.7	8.4

overlies the one of the observations, but e4 is still biased similarly as in Fig. 4. From Table 3 showing bias and RMSE, we see that the bias has improved by a degree in most temperature regions for most seasons. The low RMSEs indicate good synchronic match. An exception is the winter season, where the extreme temperatures are poorest simulated. However, for region 2 (southwestern coast), the RMSE for winter is rather low. This may be explained by this region’s marine character, inhibiting low temperatures.

3.4 Wind: point measurements

The overall best improvements comparing to the reference, may be on the coastal wind stations. Low and moderate winds (<12–15 m/s) are very well simulated, while e4 winds have a rather poor representation. A demonstrative

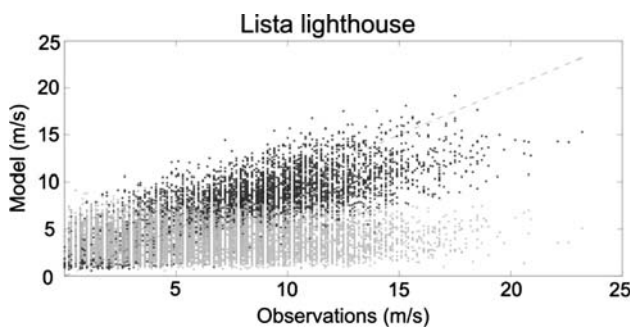


Fig. 5 Scatterplot of daily wind for light house station Lista at the south tip of Norway. Dark dots are ArpN and light dots are e4. The ‘glitches’ in the dataset is due to assignment to wind class (manual observations)

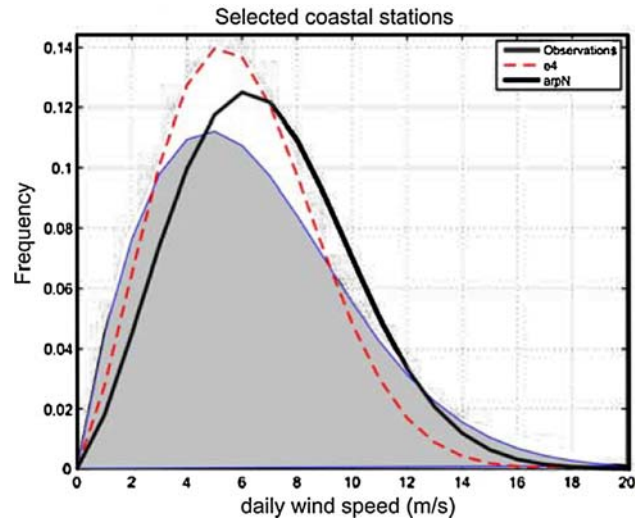


Fig. 6 Fitted Weibull distribution for daily wind observations (gray), arpN (solid) and e4(dashed) for selected coastal station, whole year

example is seen on Fig. 5 showing scatter plot for Lista light house, at the south tip of Norway. We found the moderate winds to greatly improve. Figure 6 shows a Weibull fitted distribution for the three datasets. For low and moderate values, arpN over-exaggerates a little, while for higher values, arpN perform well. This is manifested by values in Table 4 showing over- and underestimation at 90 percentile and 99.9 percentile level. For instance, arpN has a 10–15% underestimation at the higher level (99.9 percentile). Furthermore, the winter season has the largest RMSE. This may be explained by larger amplitudes in the winter data, and thus a bigger chance for errors at large values, favoring a larger RMSE. Verification of inland stations shows much lower skill (not shown), and as mentioned earlier, this is due to terrain features dominated by small scales.

We have briefly looked at wind direction for the selected coastal stations, and find that the direction of southerly winds is improved in the new dataset (not shown), whereas northerly winds show no clear improvements. This may be explained by the increased terrain resolution giving a more

Table 4 Statistical measures for wind divided into four seasons for selected coastal stations

Measure	arpN				e4			
	DJF	MAM	JJA	SON	DJF	MAM	JJA	SON
Bias	0.45	0.19	0.14	0.42	-0.26	-0.31	-0.35	-0.11
RMSE	7.82	4.93	3.45	5.51	9.06	5.54	3.98	6.42
90 (%)	0	2	2	-1	-8	-7	-10	-9
99.9 (%)	-10	-9	-11	-15	-21	-19	-22	-23

The lower two rows indicate the under-/overestimation in % for 90 percentile and 99.9 percentile

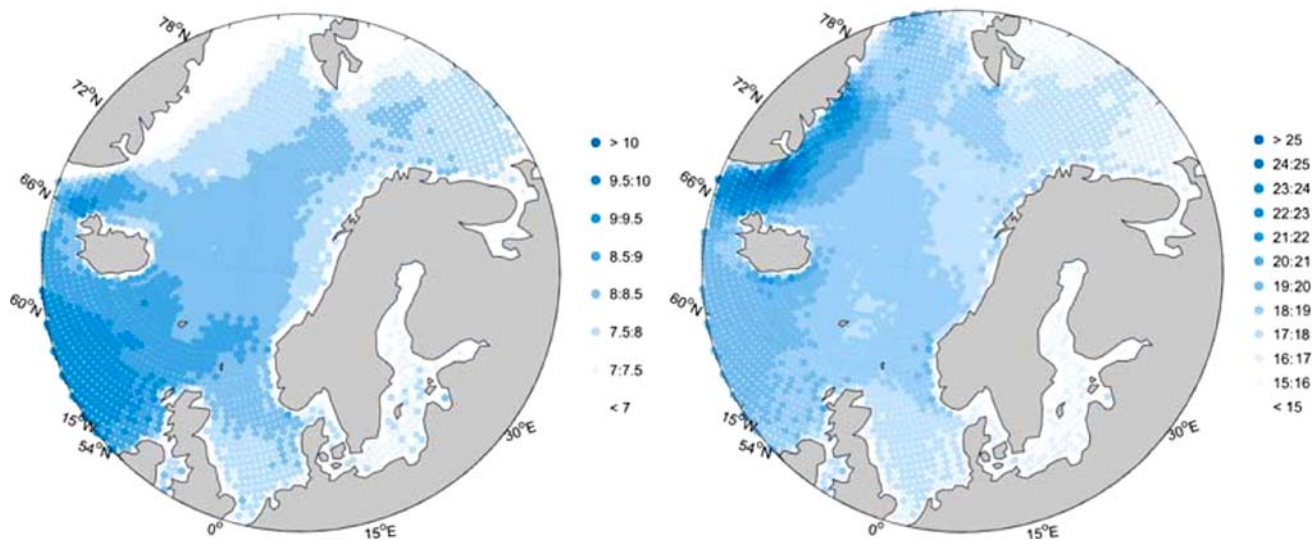


Fig. 7 Daily wind speed produced by arpN. To the left 50 percentile, to the right 99.9 percentile

correct dynamical response for the relative stronger southerly winds.

3.5 Wind: geographical distribution

The highest mean wind values in arpN are found over the ocean in a band from the northern part of the British Isles to the south tip of Svalbard, see Fig. 7. This band seems to be linked to the track of low pressure system entering the Barents Sea (Sorteberg and Walsh 2008). Both the mean and the 99.9 percentile indicate enhanced offshore winds associated with the terrain in southern Norway. Jets appearing as a response to the terrain along the southern Norway coastline have been studied by Barstad and Grønås (2005, 2006). Judging from comparison of e4 and ArpN (both the mean and 99.9 percentile; not shown), it is evident that the terrain effects—first of all showing up as coastal wind enhancements—are the most pronounced difference. Differences due to slightly different land masks in the two model systems are also present.

4 Remarks and conclusions

This paper describes the results from dynamical downscaling of the ERA40 dataset over Norway. The downscaling has been carried out by using a stretched global model with up to three times the resolution of the original ERA40. The longest waves of the ERA40 solution (longer than T42) have been nudged on to the downscaling, and consequently the results are synchronized with ERA40 and observations. The following atmospheric parameters have been compared for the period 1961–1990: daily precipitation, daily 10 m wind and daily 2 m temperature.

The results show that precipitation has significantly improved over ERA40, and that the underestimation of precipitation is about 15–25% at the 50 percentile level and a little more (~25%) for higher values (99.9 percentile). For 2 m temperature the bias in the new simulation is improved by 1°C, but still a degree warmer than observed. The wind varies a lot over land and few if any stations are representative for an area comparable to the model grid. At the coast where stations typically are more representative, we see an improvement in the simulations. However observed strong winds (above 15–20 m/s) are still too weak in the simulation. From the 10 m wind field, detailed coastal jets appear, and from the precipitation field, detailed dry spots in the interior of the southern Norway massif are reproduced.

Acknowledgments The financial support for this work has been provided by the Norwegian Research Council through the GeoExtreme project. Computer resources have been provided by the national supercomputer resources (“Notur”) and the authors appreciate the help and support from *Parallab* at the University of Bergen. This is publication no A 199 from the Bjerknes Centre for Climate Research.

References

- Barstad I, Grønås S (2005) Southwesterly flows over southern Norway—mesoscale sensitivity to large-scale wind direction and speed. *Tellus* 57A:136–152
- Barstad I, Grønås S (2006) Dynamical structures for southwesterly airflow over southern Norway—the role of dissipation. *Tellus* 58A:2–18
- Caires S, Sterl A (2003) Validation of ocean wind and wave data using triple collocation. *J Geophys Res* 108(C3):3098. doi: [10.1029/2002JC001491](https://doi.org/10.1029/2002JC001491)
- Caires S, Sterl A, Bidlot J-R, Graham N, Swail V (2004) Intercomparison of different wind wave reanalyses. *J Climate* 17(10):1893–1913

- Christensen JH, Carter TR, Giorgi F (2002) PRUDENCE employs new methods to assess European climate change. *EOS* 83:147
- Déqué M, Piedelievre JP (1995) High resolution climate simulation over Europe. *Clim Dyn* 11:321–339
- Fowler HJ, Ekström M, Blenkinsop S, Smith AP (2007) Estimating change in extreme European precipitation using a multimodel ensemble. *J Geophys Res* 112:D18104. doi:[10.1029/2007JD008619](https://doi.org/10.1029/2007JD008619)
- Giorgi F, Mearns LO (1999) Introduction to special section: regional climate modeling revisited. *J Geophys Res* 104:6335–6352
- Guldberg A, Kaas E, Déqué M, Yang S, Vester Thorsen S (2005) Reduced systematic errors by empirical model correction; impact on seasonal prediction skill. *Tellus* 57A:575–588
- Hanssen-Bauer I, Førland EJ, Tveito OE, Nordli PØ (1997) Estimating regional precipitation trends—comparison of two methods. *Nord Hydrol* 28:21–36
- Hanssen-Bauer I, Førland EJ (1998) Annual and seasonal precipitation variations in Norway 1896–1997. *KLIMA Report* 27:98, Norwegian Meteorological Institute, Oslo
- Jacob D et al (2007) An inter-comparison of regional climate models for Europe: model performance in present-day climate. *Clim Change* 81:31–52. doi:[10.1007/s10584-006-9213-4](https://doi.org/10.1007/s10584-006-9213-4)
- Jiang C, Cronin MF, Kelly KA, Thompson L (2005) Evaluation of a hybrid satellite- and NWP-based turbulent heat flux product using tropical atmosphere-ocean (TAO) buoys. *J Geophys Res* 110:C09007. doi:[10.1029/2004JC002824](https://doi.org/10.1029/2004JC002824)
- Kalnay E et al (1996) The NCEP/NCAR 40-year reanalysis project. *Bull Am Meteorol Soc* 77:437–471
- Kållberg PA, Simmons A, Uppala S, Fuentes M (2004) The ERA-40 archive, ERA-40. *Proj Rep Ser* 17:1–32
- Lorant V, Royer JF (2001) Sensitivity of equatorial convection to horizontal resolution in aqua-planet simulations with variable-resolution GCM. *Mon Wea Rev* 129:2730–2745
- Mavromatis T, Jones PD (1999) Evaluation of HadCM2 and direct use of daily GCM data in impact assessment studies. *Clim Change* 41:583–614. doi:[10.1023/A:1005336608651](https://doi.org/10.1023/A:1005336608651)
- Meinke IH, von Storch H, Feser F (2004) A validation of the cloud parameterization in the regional model SN-REMO. *J Geophys Res* 109:D13205. doi:[10.1029/2004JD004520](https://doi.org/10.1029/2004JD004520)
- Miguez-Macho G, Stenchikov G, Robock A (2004) Spectral nudging to eliminate the effects of domain position and geometry in regional climate model simulations. *J Geophys Res* 109:D13104. doi:[10.1029/2003JD004495](https://doi.org/10.1029/2003JD004495)
- Miguez-Macho G, Stenchikov G, Robock A (2005) Regional climate simulations over North America: interaction of local processes with improved large-scale flow. *J Climate* 18:1227–1246
- Schmidli J, Frei C, Vidale PL (2006) Downscaling from GCM precipitation: a benchmark for dynamical and statistical downscaling methods. *Int J Climatol* 26(5):679–689
- Schmidli J, Goodess CM, Frei C, Haylock MR, Hundecha Y, Ribalaygua J, Schmith T (2007) Statistical and dynamical downscaling of precipitation: an evaluation and comparison of scenarios for the European Alps. *J Geophys Res* 112:D04105. doi:[10.1029/2005JD007026](https://doi.org/10.1029/2005JD007026)
- Smith SR, Legler DM, Verzone KV (2001) Quantifying uncertainties in NCEP reanalyses using high quality research vessel observations. *J Clim* 14:4062–4072
- Sorteberg A, Walsh J (2008) Seasonal Cyclone Variability at 70°N and its impact on moisture transport into the Arctic. *Tellus* 60A:570–586
- Tveito OE, Bjørndal I, Skjelvåg AO, Aune B (2005) A GIS-based agro-ecological decision system based on gridded climatology. *Meteorol Appl* 12:57–68. doi:[10.1017/S1350482705001490](https://doi.org/10.1017/S1350482705001490)
- von Storch H, Langenberg H, Feser F (2000) A spectral nudging technique for dynamical downscaling purposes. *Mon Wea Rev* 128:3664–3673
- Vukicevic T, Errico R (1990) The influence of artificial and physical factors upon predictability estimates using a complex limited-area model. *Mon Wea Rev* 118:1460–1482
- Wilby RL, Wigley TML, Conway D, Jones PD, Hewitson BC, Main J, Wilks DS (1998) Statistical downscaling of general circulation model output: a comparison of methods. *Water Resour Res* 34:2995–3008
- Waldron KM, Peagle J, Horel JD (1996) Sensitivity of a spectrally filtered and nudged limited area model to outer model options. *Mon Wea Rev* 124:529–547
- Weisse R, Feser F (2003) Evaluation of a method to reduce uncertainty in wind hindcasts performed with regional atmosphere models. *Coast Eng* 48:211–225
- Yuan X (2004) High wind speed evaluation in the Southern Ocean. *J Geophys Res*, 109(D3): Art. No. D13101